

Maximum Allowable Current Determination of RBS By Using a Directed Graph Model and Greedy Algorithm

Binghui Xu^{1†}, Guangbin Hua^{1†}, Cheng Qian^{1*}, Quan Xia^{1,2}, Bo Sun¹, Yi Ren¹, and
Zili Wang¹

¹School of Reliability and Systems Engineering, Beihang University, Beijing, 100191,
China

²School of Aeronautic Science and Engineering at Beihang University, Beijing, China

*Address correspondence to: cqian@buaa.edu.cn

†These authors contributed equally to this work.

Abstract

Reconfigurable ~~Battery Systems~~ battery systems (RBSs) present a promising alternative to traditional battery systems due to their flexible and dynamically changeable topological structure ~~subjected to that can be adapted to different~~ battery charging and discharging strategies. During ~~the operation of the RBS, the Maximum Allowable Current~~ RBS operation, a critical system parameter known as the maximum allowable current (MAC) ~~of system that ensures each battery's current remains become pivotal. This parameter is instrumental in maintaining the current of each individual battery within a safe range, is a critical indicator to guide the system's reconfiguring control, and serves as a guiding indicator for the system's reconfiguration, thereby ensuring its safety and reliability. In this paper, we firstly propose a calculation method for~~ This paper proposes a method to calculate the MAC of arbitrary ~~RBS~~ RBSs using a greedy algorithm in conjunction with a directed graph model of the RBS. ~~In this method, a new directed graph model is developed to model the structure of RBS, and a greedy algorithm is designed to find the possible circuit that enable MAC. Then, the MAC is calculated~~ By introducing the shortest path of the battery, the greedy algorithm transforms the enumeration of switch states in the brute-force algorithm into the combination of the shortest paths, which greatly increases the efficiency with which the MAC is determined. The directed graph model, based on the circuit in-cooperate with the equivalent model of batteries and switches. The effectiveness of the equivalent circuit, provides a specific method for calculating the MAC of a given structure. The proposed method is validated ~~by a novel and complex RBS on two published four-battery-RBSs and one with a more complex structure. The results show that this method is capable to calculated~~ are the same as those of the brute-force algorithm, but the proposed method significantly improves the computational efficiency ($N_s 2^{N_s - N_b} \log_{10} N_b$ times faster than the brute force algorithm for an RBS with N_b batteries and N_s switches, theoretically). The main advantage of the proposed method is its ability to calculate the

MAC of RBSs with ~~different structures or different battery sizes efficiently, which proves the correctness of this method and its potential in facilitating next-generation RBS designs and applications, including battery isolation.~~ arbitrary structures, even in scenarios with random isolated batteries.

1 Introduction

Battery ~~Energy Storage Systems~~ energy storage systems (BESSs) are extensively ~~employed~~ used in various applications [1], such as wind power plants [2] and space power systems [3, 4], to store and release high-quality electrical energy [2, 1, 5, 4, 3][5]. Typically, a BESS consists of numerous batteries interconnected by series-parallel circuitry to provide the required capacity storage. However, traditional BESSs, in which the batteries are connected in a fixed topology, ~~exhibit~~ suffer from a significant weakness in their worst battery due to the so-called cask effect. Moreover, if ~~this the~~ worst battery fails during operation, it ~~can~~ is highly likely to exacerbate the degradation of ~~other batteries with a high possibility~~ the other batteries, leading to reliability and safety issues [6, 7, 8]. These problems have become significant technical barriers in ~~the development of many engineering projects requiring high reliability, such as developing~~ new-generation space vehicles ~~and urgently need to be addressed~~ [9].

Reconfigurable ~~Battery System (RBS)~~ battery systems (RBSs), which can dynamically switch ~~as required~~ to different circuit topology configurations as required, is ~~topologies, are~~ expected to solve ~~the above problems~~ this problem [10]. The ~~ability of~~ switching circuit helps to isolate unhealthy batteries, ~~and thereby improve~~ thereby improving the safety and reliability of the battery system. ~~Figure 1a shows~~ To illustrate the working principle of an RBS, we consider a typical RBS structure developed by Visairo [11] ~~for dynamically adjusting the output voltage and current~~ (Fig. 1a), which is taken as an example to show the reconfiguration process. In this structure, the batteries can be connected not only in series when the switches S_1 , S_5 , S_6 , S_7 , S_8 , S_9 , and S_{13} are closed (~~Figure 1b~~), ~~see Fig. 1b~~ but also in parallel when S_1 , S_2 , S_3 , S_4 , S_5 , S_9 , S_{10} , S_{11} , S_{12} , and S_{13} are closed (~~Figure Fig. 1c~~). Furthermore, when an unhealthy battery, for instance, the orange one B_3 in ~~Figure Fig. 1d~~, appears in the RBS, it can be isolated by opening its two adjacent switches (i.e., S_4 and S_{11}), ensuring ~~the system still remains that the system remains in~~ a reliable working mode.

~~The complex connection~~ Recently, various types of RBSs with different flexibility and reconfigurability have been designed to meet application requirements. For example, Ci et al. [12] proposed an RBS structure that dynamically adjusts the battery discharge rate to fully exploit the available capacity of each battery. Jan's [13, 14] structures reconfigure structures with variant batteries in series to reach the (constantly changing) voltage requirements during electric vehicle charging. As shown in Fig. 1a, the structure proposed by Visairo et al. [11] changes the system's output voltage based on the load conditions, thereby reducing the power loss of the voltage regulator during the power supply process and improving the efficiency of energy use. Also, to enhance the energy efficiency of the system, Lawson et al. [15] and He et al. [16] proposed simplified structures that have fewer switches than Visairo's design. Kim et al. [17] improved the system's ability to recover from battery failures by introducing multiple ports into the structure.

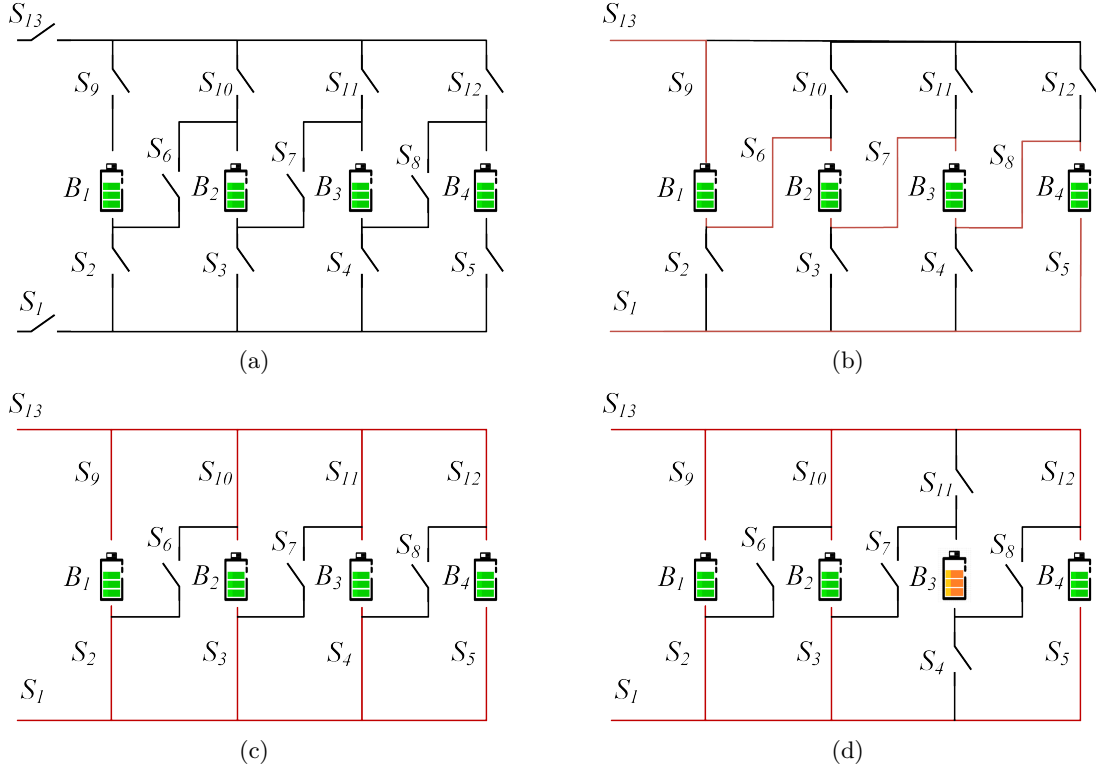


Figure 1: (a) The RBS structure proposed by Visairo[11], with all batteries in (b) series connection, (c) parallel connection, and (d) battery B_3 isolated.

The complex structure between batteries and switches in the RBS provides gives RBSs flexibility but also introduces challenges in design and operational control. Unlike traditional BESSs with fixed outputs, the RBS output must be dynamically adjusted by controlling switch states to meet external load requirements. This necessitates additional, time-consuming output performance analysis during design and corresponding control strategies. An incorrect switch control strategy may cause battery short-circuiting or overload, risking the entire system. The Maximum Allowable Current creates challenges in the design and control of the system. Thus, several approaches to analyze the RBS structure and performance have been proposed to tackle these challenges. For instance, Han et al. [18] derived an analytical expression for the maximum switch current during battery system reconfiguration for a specific RBS structure. This helps guide the selection of switches and supports the design of RBS hardware. Chen et al. [19] proposed a systematic approach based on sneak circuit theory to fundamentally avoid the short-circuit problem of RBSs: They thoroughly analyzed all paths between the cathode and anode of each battery in the RBS and identified paths that only contain switches as short-circuit paths for pre-checking before system reconfiguration.

In spite of the maximum switch current mentioned above, the maximum allowable current (MAC), an RBS performance indicator, can guide designers in addressing this issue. MAC is defined as the maximum RBS output current that ensures each battery's current remains within a safe range. Therefore, it provides a benchmark for RBS output current, protecting individual batteries and identifying overall system output limits during operation. Despite its importance, no method currently exists for automatically evaluating MAC for RBSs. In particular, when one or more random cells are isolated, there is still no method to determine the MAC of the remaining RBS in time to assist the system in adjusting the control strategy timely. A universal and automatic method for calculating RBS MAC is urgently needed for practical applications. In this study, a directed graph model and greedy algorithm are employed to determine the MAC of RBS and the corresponding control strategy, effectively calculating the MAC for allowed current under the constraints of the battery cell, is another critical indicator of RBSs that needs to be evaluated during the design or control of the system. The MAC helps the designers assess whether the RBS meets the output current requirements and contributes to the formulation of appropriate and safe management strategies for the battery management system. Unfortunately, few studies have analyzed the RBS structure to determine the RBS MAC. An intuitive and straightforward method is to enumerate all possible switch states and calculate the output current of the system under each reconfigured structure. However, this method is inefficient and time-consuming, especially for RBSs with a large number of switches.

To solve this issue, this paper proposes an efficient method to evaluate the MAC of RBSs. In this method, a greedy algorithm is designed to efficiently search the possible circuit topology of RBSs with MAC. This algorithm transforms the enumeration of switch states in the brute-force algorithm into the combination of the batteries' shortest paths. An improved direct graph model that considers the voltage, the internal resistance, the MAC of the battery, and the external load is also introduced to analyze the current of the RBS. The main contributions of this paper can be summarized as follows:

- An efficient method is proposed to determine the MAC of RBSs with arbitrary structures,

including scenarios with isolated batteries.

- A greedy algorithm is applied to solve the MAC problem, the computational complexity of which is greatly reduced compared with the brute-force algorithm.
- An improved directed graph model is introduced to provide a specific method for calculating the MAC of a given structure.

The remainder of this paper is organized as follows: Section II presents the framework and details of the proposed directed graph model and the greedy algorithm. Section III demonstrated discusses a case study of using that uses the proposed method to determine the MAC of a novel and MACs of two published four-battery RBSs and one with a more complex structure. The calculation results, the algorithm's computational complexity, and scenarios such as batteries isolation also are battery random isolation are also discussed. Finally, the concluding remarks are drawn presented in Section IV.

2 Methodology

The central principle of this method is to make connect the batteries in RBS connected in parallel as much as an RBS in parallel to the extent possible, thereby maximizing the output current of the RBS. To achieve this universally and automatically achieve this, the overall process is divided into four steps, as shown in Figure 2. Firstly the four steps shown in Fig. 2. First, a directed graph model is established for subsequent computing, which computations. The model not only contains the connected relationships between batteries and switches, but also retains the performance parameters of the batteries. Subsequently, based on the equivalent circuit, the MAC problem is transformed into specific objective functions and constraints. Then, the The shortest paths (SPs, where additional batteries and switches on the path are penalized as distance) for the batteries are obtained then obtained by using the Dijkstra algorithm to guide connect the batteries in the RBS connect in parallel. Finally, a greedy algorithm is employed used to organize the switches, allowing the batteries to connect via their SPs while satisfying the constraints, resulting in the MAC of the RBS.

2.1 Directed graph Model model

He et al. [20] once proposed an abstracted directed graph model for an RBS, where the nodes represented represent the batteries, the edges represented represent the configuration flexibility, and the weight of each vertex corresponded corresponds to the battery voltage (Figure Fig. 3a). The model effectively captured captures all potential system configurations and offered offers a direct metric for configuration flexibility, but it did does not specify the physical implementation of the connectivity between batteries, meaning that one graph might have had correspond to multiple RBS structures. We previously proposed a novel directed graph model that, in contrast to differs completely from He's model, used by using nodes to represent the connections between batteries and switches, and directed edges to represent batteries and switches (Figure Fig. 3b), allowing for a one-to-one correspondence between the RBS structure and the directed graph model. This model

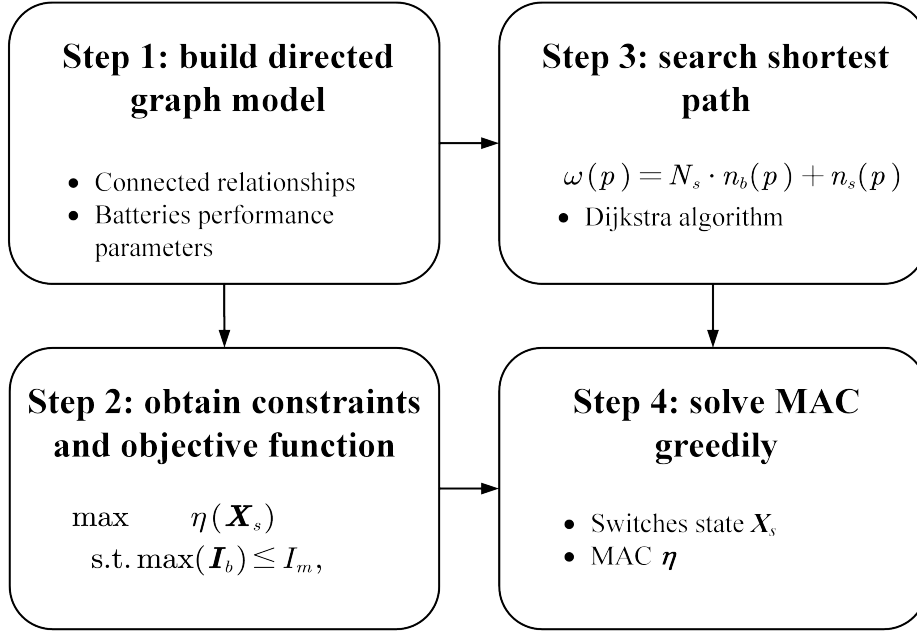


Figure 2: Diagram of this method, which contains four main steps.

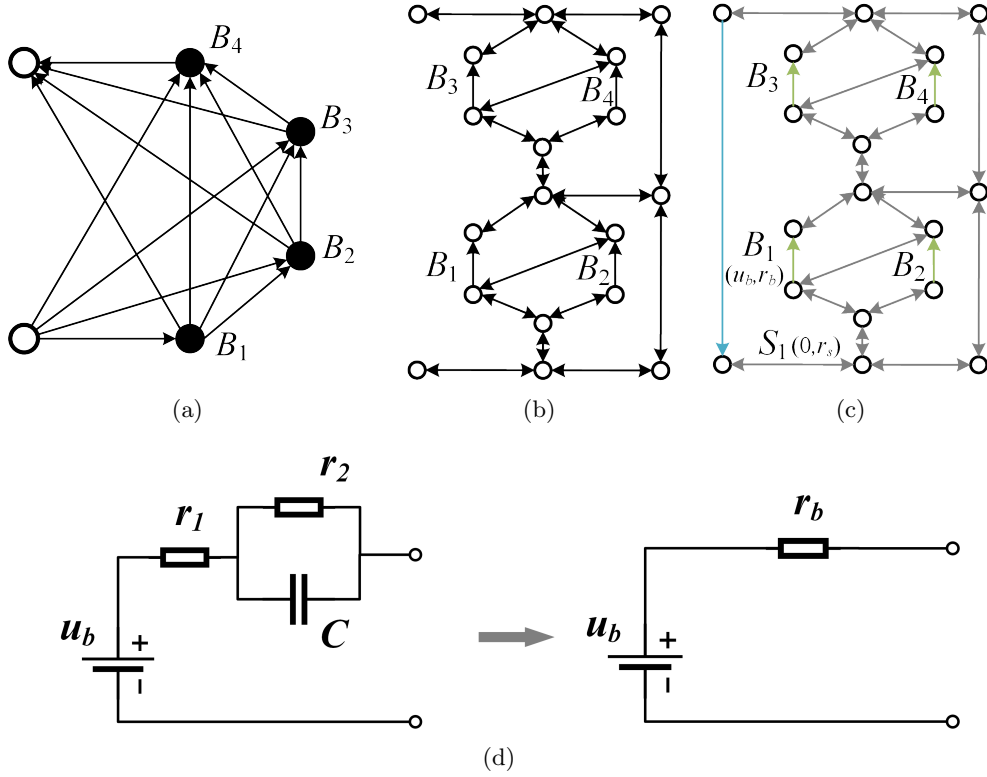


Figure 3: Directed graph models used in (a) He's work [20], (b) our previous work, and (c) [the improved model in](#) this paper. (d) The equivalent circuit of a battery in this method.

was able to accurately and comprehensively represent the RBS topological structure but could not be used for quantitative MAC calculations due to the lack of consideration for battery and switch performance parameters because it does not consider the voltage, internal resistance, and MAC of the battery. To address this, an improved directed graph model is used here based on our original model. issue, we improve our previous model by adding electromotive force and resistance attributes on the edges based to equivalent circuits (Figure 3e) on its equivalent circuits. The model also considers the external load as an equivalent resistance and integrate it into the analysis, making it a complete circuit model for later circuit analysis. The following will provide analyses. Fig. 3c shows the improved directed graph model used in this paper. The following provides a detailed explanation of the method for equating the components in RBS components in RBSs and constructing the directed graph model.

In order to use circuit analysis methods to solve the MAC of the RBS, the components in the RBS are equated to ideal circuit elements. As shown in Figure 3d, the battery in the RBS can be represented as a black-box circuit consisting of two resistors (r_1 and r_2) and a capacitor (C), known as the Thevenin model [21, 22]. With an emphasis on the stable output of the RBS, the capacitor in the Thevenin model can be considered as an open circuit without affecting the steady-state current. Therefore, the battery B_i in the RBS can be simplified as a series connection between a constant voltage source u_i and a resistor r_i . Furthermore, the state of switch S_j in the RBS is represented by a binary variable x_j , where 0 is for ON and 1 is for OFF, respectively. When the switch is closed, it can be regarded as a resistor with a very small resistance value r_j . Lastly, the external load is considered as a resistor with a value of resistance R_o .

For a given RBS structure, its directed graph model for the RBS $G(V, E)$ is constructed as a directed graph $G(V, E)$ in such a way that follows:

1. Nodes: The nodes in the directed graph correspond to the connection points of components in the actual RBS. Assuming there are a total of N nodes in the RBS, for the sake of convenience, the anode of the RBS is denoted as v_1 and the cathode as v_N .
2. Edges: The edges in the directed graph correspond to the batteries, switches, and external electrical loads in the actual RBS. Therefore, there are three types of directed edges. For a battery B_i , its directed edge e_i is drawn from the cathode to the anode, as the battery because the battery in operation only allows current to flow in one direction when in operation. For a switch S_j , since it is allowed to work under bi-directional currents, it is represented by a pair of directed edges with two-way directions. Regarding the external electronic load, as because it is connected to the anode and cathode of the RBS, a directed edge from v_N to v_1 is used to represent it. In conclusion, for a given RBS structure with N_b batteries and N_s switches, the total number of directed edges is $N_b + 2N_s + 1$, where 1 refers to the external electrical load.
3. Edges' attributes: Each edge is assigned two attributes, voltage difference and resistance, based on the equivalent method mentioned above. The values for the battery B_i , switch S_j , and external loads correspond to (u_i, r_i) , $(0, r_j)$, and $(0, R_o)$, respectively.

2.2 Constraints and Objective Function

Based on the definition of MAC, determining the MAC of RBS For a given RBS, determining its MAC involves maximizing the RBS output current while ensuring that the currents of all batteries all battery currents do not exceed the batteries' maximum allowable current. In this subsection, MAC. This subsection establishes the constraints and objective function to solve-determine the RBS's MAC will be established through circuit analysis, based on the previously constructed directed graph model provided in the previous section.

First, the topology in the directed graph model is represented in matrix form \mathbf{A} , known as the incidence matrix, to facilitate circuit analysis. The specific definition of the incidence matrix is shown in Equation 1, and defined as follows:

$$a_{kl} = \begin{cases} 1, & \text{edge } l \text{ leaves node } k, \\ -1, & \text{edge } l \text{ enters node } k, \\ 0, & \text{otherwise.} \end{cases} \quad (1)$$

For a directed graph consisting of N nodes and $N_b + 2N_s + 1$ directed edges, its incidence matrix \mathbf{A} is an $N \times (N_b + 2N_s + 1)$ matrix. In this matrix, the rows and columns represent the nodes and edges of the directed graph, respectively. By distinguishing the components in the RBS corresponding to each column, \mathbf{A} can be rewritten as :-

$$\mathbf{A} = \begin{bmatrix} \mathbf{A}_b & \mathbf{A}_s & \mathbf{A}_o \end{bmatrix}, \quad (2)$$

where \mathbf{A}_b , \mathbf{A}_s , and \mathbf{A}_o are the sub-matrices corresponding to the batteries, switches, and external electrical load, respectively. To alleviate-reduce the computational complexity, the dimensions of matrix \mathbf{A} undergoes dimensionality reduction are reduced. Since each directed edge has one node to leave and one to enter, the sum-of-the-values in every column of \mathbf{A} is sum to zero. Therefore removing any single one, removing the last row will not result in a loss of information. Without loss of generality, the last row is removed here. On the other hand, Conversely, since each switch in the RBS is represented by a pair of directed edges with two-way directions, the two columns corresponding to the switch are mutually opposite. Thus, for the sub-matrix submatrix \mathbf{A}_s , only one column is retained for each pair of columns representing the same switch. As a result, \mathbf{A} can be reduced to a $(N - 1) \times (N_b + N_s + 1)$ matrix, denoted as $\tilde{\mathbf{A}}$, for further calculation of current and voltage. Similar to Equation-2 Eq. (2), $\tilde{\mathbf{A}}$ can be rewritten as :-

$$\tilde{\mathbf{A}} = \begin{bmatrix} \tilde{\mathbf{A}}_b & \tilde{\mathbf{A}}_s & \tilde{\mathbf{A}}_o \end{bmatrix}. \quad (3)$$

After obtaining the incidence matrix, the currents of all batteries and output in the RBS are

217 determined by solving the circuit equations. According to ~~Kirchhoffs law~~Kirchhoff's laws, we have

$$\begin{cases} \tilde{\mathbf{A}}\mathbf{I} = \mathbf{0}, \\ \mathbf{U} = \tilde{\mathbf{A}}^T\mathbf{U}_n, \end{cases} \quad (4)$$

218 where \mathbf{I} and \mathbf{U} indicate the current and voltage difference arrays of the $N_b + N_s + 1$ edges, respectively;
219 and \mathbf{U}_n is the voltage array of the $N - 1$ nodes. These directed edges are treated as generalized
220 branches and expressed in matrix form as follows:

$$\mathbf{I} = \mathbf{Y}\mathbf{X}\mathbf{U} - \mathbf{Y}\mathbf{X}\mathbf{U}_s + \mathbf{I}_s, \quad (5)$$

221 where \mathbf{U}_s and \mathbf{I}_s denote the source voltage and source current of the generalized branches, respec-
222 tively. Because all batteries have been equivalent to voltage sources rather than current sources
223 in the previous subsection, all elements of the array \mathbf{I}_s are ~~0, while zero,~~ zero, whereas the elements of
224 the array \mathbf{U}_s are equal to the first attribute of the corresponding edges in the directed graph. The
225 matrix \mathbf{Y} in ~~5-Eq. (5)~~ is the admittance matrix of the circuit ~~and is~~ defined as the inverse of the
226 impedance matrix. ~~That is the elements of the diagonal~~ The elements on the diagonal of matrix
227 \mathbf{Y} are equal to the reciprocal of the resistance, which is the second attribute of the corresponding
228 edges in the directed graph~~and the~~. The off-diagonal elements are 0. The of \mathbf{Y} are zero. \mathbf{X} is the
229 state matrix ~~which describes that determines~~ whether the RBS batteries and switches ~~are allowed~~
230 to can pass current. It is defined as

$$\mathbf{X} = \text{diag}(\underbrace{1, 0, \dots, 1}_{N_b \text{ of } 0/1}, \underbrace{1, 0, \dots, 1}_{N_s \text{ of } 0/1}, 1) = \begin{bmatrix} \mathbf{X}_b & & \\ & \mathbf{X}_s & \\ & & 1 \end{bmatrix}, \quad (6)$$

231 ~~Where the elements~~ where element x_i of the matrix \mathbf{X}_b ~~represent whether the battery i indicates~~
232 whether battery B_i has been removed from the circuit, with $x_i = 1$ indicating removal and $x_i = 0$
233 indicating that it battery B_i is still available to supply power. When all batteries are ~~health~~ healthy
234 and capable of providing current to the external load, \mathbf{X}_b is ~~an the~~ identity matrix. The elements
235 x_j of the matrix \mathbf{X}_s ~~represent whether the switch j determine whether switch S_j is closed,~~
236 $x_j = 1$ indicating ~~closure~~ a closed switch and $x_j = 0$ indicating ~~disconnection~~ an open switch, which
237 is consistent with the previous subsection.

238 Theoretically, the output current I_o and the currents of each battery \mathbf{I}_b in the RBS can be
239 determined by solving ~~Equations 4, 5, and 6~~ Eqs. (4)–(6) under any given state \mathbf{X} . ~~In order to~~
240 ~~obtain specific constraint conditions and objective functions~~ To further simplify the problem, it is
241 ~~further~~ assumed that all batteries have the same electromotive force and internal resistance, ~~denoted~~
242 ~~as which are denoted~~ u_b and r_b , respectively. This allows ~~for the derivation of us to derive~~ explicit
243 expressions for I_o and \mathbf{I}_b . After derivation and simplification, the output current I_o and the currents
244 of each battery \mathbf{I}_b are ultimately represented as ~~Equations 7 and 8, respectively.~~ Eqs. (7) and (8).

respectively:

$$I_o = \frac{1}{R_o r_b} \tilde{\mathbf{A}}_o^T \mathbf{Y}_n^{-1}(\mathbf{X}) \tilde{\mathbf{A}}_b \mathbf{U}_b, \quad (7)$$

$$\mathbf{I}_b = \frac{1}{r_b^2} [\tilde{\mathbf{A}}_b^T \mathbf{Y}_n^{-1}(\mathbf{X}) \tilde{\mathbf{A}}_b \mathbf{U}_b - r_b \mathbf{U}_b], \quad (8)$$

where \mathbf{U}_b is an $N_b \times 1$ array with all elements equaling equal to u_b , and \mathbf{Y}_n is the equivalent admittance matrix of the circuit, and is defined as

$$\mathbf{Y}_n(\mathbf{X}) = \frac{1}{R_o} \tilde{\mathbf{A}}_o \tilde{\mathbf{A}}_o^T + \frac{1}{r_b} \tilde{\mathbf{A}}_b \mathbf{X}_b \tilde{\mathbf{A}}_b^T + \frac{1}{r_s} \tilde{\mathbf{A}}_s \mathbf{X}_s \tilde{\mathbf{A}}_s^T. \quad (9)$$

To characterize the current output capacity of the RBS structure under different switching states, an indicator η is defined by the ratio of I_o and to $\max(\mathbf{I}_b)$ shown in Equation 10:

$$\eta = \frac{I_o}{\max(\mathbf{I}_b)}. \quad (10)$$

Finally the problem of solving finding the MAC can be formulated as

$$\max \eta(\mathbf{X}_s) \quad (11)$$

$$\text{s.t.s.t.} \quad \max(\mathbf{I}_b) \leq I_m, \quad (12)$$

where I_m is the maximum allowable current MAC of the battery.

However, it is remains computationally difficult to solve 11 because of the Eq. (11) because of \mathbf{Y}_n^{-1} . On one hand, due to the introduction of nonlinear terms by \mathbf{Y}_n^{-1} , many effective renders many methods in linear optimization are not suitable unsuitable for this problem. On the other hand, the rank of \mathbf{Y}_n is proportional to the number of batteries and switches, which can be very large for a large RBS system, leading to a significant computational burden. Therefore As a result, intelligent algorithms that rely on evolving evolution by iteration may face efficiency issues problems when dealing with large RBS system. In order to a large RBS. To address this issue, the problem should be considered from the perspective of guiding the RBS to reconstruct as many parallel structures as possible. Consequently, a greedy algorithm based on the shortest path is proposed. The detailed implementation process of this algorithm is presented in the following two subsections.

2.3 Shortest Pathpath

The path p used in this method is defined as the complete route that passes through one battery (or a consecutive series of batteries) and closed switches, connecting the anode v_1 to the cathode v_N of the RBS. By applying a penalty to the series-connected batteries on the path, where additional batteries imply a longer greater distance, the algorithm encourages the RBS to form parallel structures as much as possible. Meanwhile to the extent possible. In addition, to reduce the number of switches controlled during the reconstruction process, a penalty is also applied to the total number of switches on the path, while ensuring the minimum number of batteries. Therefore, the distance ω of the

271 path p is defined by the following equation:

$$\omega(p) = N_s \cdot n_b(p) + n_s(p), \quad (13)$$

272 where N_s is the total number of switches in the system, and $n_b(p)$ and $n_s(p)$ are number of batteries
273 and switches in the path p , respectively. Moreover, the shortest path SP_i is defined as the path with
274 the minimum ω for battery i , as shown in the following equation:

$$SP_i = \arg \min_{p \in P_i} \omega(p), \quad (14)$$

275 where P_i is the set of all paths from v_1 to v_N which pass through the that pass through directed
276 edge i .

277 The SP_i can be solved by the Dijkstra algorithm. The Dijkstra algorithm is a graph-search
278 graph-search method that finds the shortest path between two given nodes in a weighted graph,
279 efficiently solving the single-source shortest-path problem. Assuming that shortest-path problem.
280 Denoting the cathode and anode of battery i are denoted B_i as v_i^- and v_i^+ respectively, the then
281 path p of battery i B_i can be divided into three segments: $v_1 \rightarrow v_i^-$, $v_i^+ \rightarrow v_N$, and $v_i^- \rightarrow v_i^+$. The
282 $v_i^- \rightarrow v_i^+$ is the directed edge corresponding to battery i B_i . With the Dijkstra algorithm, shortest
283 paths for the $v_1 \rightarrow v_i^-$ and $v_i^+ \rightarrow v_N$ can be calculated under the weights given in Equation 13,
284 denoted as Eq. (13) and denoted $SP(v_i^- \rightarrow v_i^+)$ and $SP(v_i^+ \rightarrow v_N)$, respectively. Finally, the SP_i
285 for battery i B_i is formed by the complete path with, which consists of $SP(v_1 \rightarrow v_i^-)$, $v_i^- \rightarrow v_i^+$,
286 and $SP(v_i^+ \rightarrow v_N)$.

277 2.4 Greedy Algorithm

278 From the perspective of series vs parallel connections, integrating more batteries into the circuit
279 through their shortest paths (SPs) results in a larger number of more batteries connected in
280 parallel, thereby increasing the total output current of the RBS. However, conflicts may arise be-
281 tween the SPs of different batteries. For instance, the SPs of two batteries might form
282 a short-circuited short-circuit RBS structure, which is not allowed. To address this issue, a greedy
283 algorithm is employed to incorporate as many SPs incorporates as many SPs as possible while
284 satisfying the reconstruction requirements.

285 The algorithm, as illustrated in Figure 4, can be (see pseudo-code in Algorithm 1) is illustrated
286 in Fig. 4 and is summarized as follows, with the corresponding pseudo-code presented in Algorithm
287 1. First, the shortest paths (SPs) are obtained using Equations 13 and 14 SPs are obtained by using
288 Eqs. (13) and (14) in conjunction with Dijkstra Search the Dijkstra search. Next, the matrix \mathbf{A} is
289 calculated using Equation 1 Eq. (1), and the initial N_{set} is set to N_b . The algorithm iteratively
290 checks uses a dichotomy method to iteratively check until convergence different combinations of c_b
291 batteries from N_b and updates N_{set} using a dichotomy method until convergence is reached N_{set} .
292 For each combination, the algorithm constructs an effective solution if possible, and calculates the
293 currents I_o and I_b using Equations 7 and 8 by using Eqs. (7) and (8). If the maximum current I_b is
294 less than or equal to I_m , the η is calculated using Equation 10 by using Eq. (10), and the maximum

305 η is updated accordingly. Finally, the algorithm outputs the maximum η once N_{set} converges.

306 3 Case Study

307 3.1 Structures

308 Currently, two types of RBS structures have been proposed by Visairo et al. [11] and Lawson et al.
309 [15], both of which have ~~been applied in practice~~ seen real use. The primary goal of Visairo's structure
310 (~~Figure 5b~~) ~~was to achieve dynamic adjustment of RBS output~~; ~~however~~ Fig. 5b is to dynamically
311 adjust the RBS output power. However, the isolation of unhealthy batteries ~~was~~ is not sufficiently
312 addressed. ~~When batteries need to be isolated in the RBS of Visairo's structure, the methods~~
313 ~~for isolating them and the subsequent changes in RBS output warrant further investigation in their~~
314 ~~work~~. Lawson et al. ~~conducted research on battery isolation in RBS and specifically designed the~~
315 ~~designed the RBS~~ structure shown in ~~Figure 5a~~. This structure has the advantage of easily isolating
316 ~~batteries, but Fig. 5a to isolate batteries~~. Although this structure easily isolates batteries, it cannot
317 dynamically adjust the output current of ~~the~~ RBS. Based on the structures of Visairo and Lawson,
318 this paper ~~presents a new structure~~, ~~as shown in Figure 5c, which combines the advantages of~~
319 ~~both~~ proposes the structure shown in Fig. 5c. By integrating the Visairo RBS structure into the
320 Lawson RBS structure, the ~~new proposed~~ structure not only ~~allows~~ has the flexibility to switch
321 the batteries between series, parallel, and mixed series-parallel modes, ~~but also easily enables~~ but
322 also allows the isolation of highly degraded batteries from the RBS. ~~And their variations in output~~
323 ~~current under battery isolation conditions will be studied~~. This RBS structure will be used to
324 ~~validate the effectiveness of the proposed method for calculating the MAC, and be compared with the~~
325 ~~Lawson's and Visairo's structure to illustrate its advantage on battery isolation~~ These four battery
326 RBS structures are investigated in the case study, including the scenarios with random isolated
327 batteries.

328 3.2 Result

329 As shown in ~~Figure Fig.~~ Fig. 5c, the new RBS structure consists of ~~4~~ four batteries and 19 switches. ~~The~~
330 Figure 6a shows the corresponding directed graph ~~is depicted in Figure 6a~~, which is composed of ~~of~~
331 ~~a total of~~ 18 nodes and 43 edges. Batteries B_1 , B_2 , B_3 , and B_4 are denoted by green directed edges
332 in the graph, ~~while and~~ the 19 switches are represented by gray directed edges with ~~bi-directional~~
333 bidirectional arrows. The external electrical load is treated as a directed edge from the cathode of
334 the RBS (i.e., node 18) to the anode (i.e., node 1), as indicated by the blue directed edge in the
335 graph. ~~Utilizing Equation 13~~ Using Eq. (13) and the Dijkstra algorithm, the ~~SPs~~ SPs of the four
336 batteries in the RBS structure of ~~Figure Fig.~~ Fig. 5c are highlighted ~~by red in Figures 6b~~ in red in Figs.
337 6b and 6e. Finally, the ~~MAC calculation results~~ calculated MACs of the structure in ~~Figure 5c~~ are
338 ~~shown as Table 1 and Figure 6f~~, Fig. 5c are listed in Tab. 1 and shown in Fig. 6f, as obtained by
339 the greedy algorithm 1. ~~Table Tab.~~ Tab. 1 contains the ~~switches states~~ states of the switches, the output
340 current I_o , ~~the~~ the battery current I_b , ~~and~~, and the ratio η of the RBS structure with all batteries in good

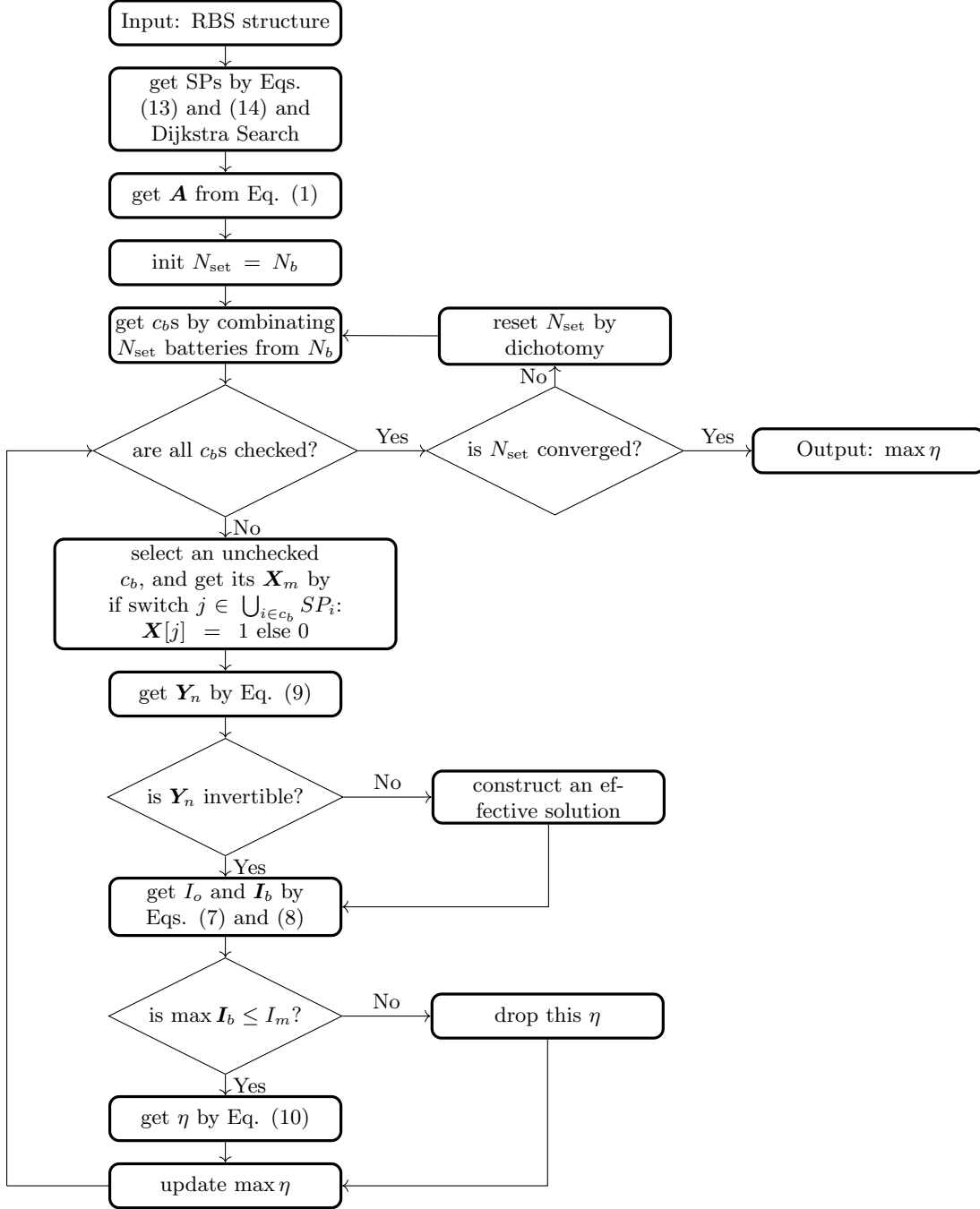


Figure 4: The computational flowchart of the MAC for a given RBS.

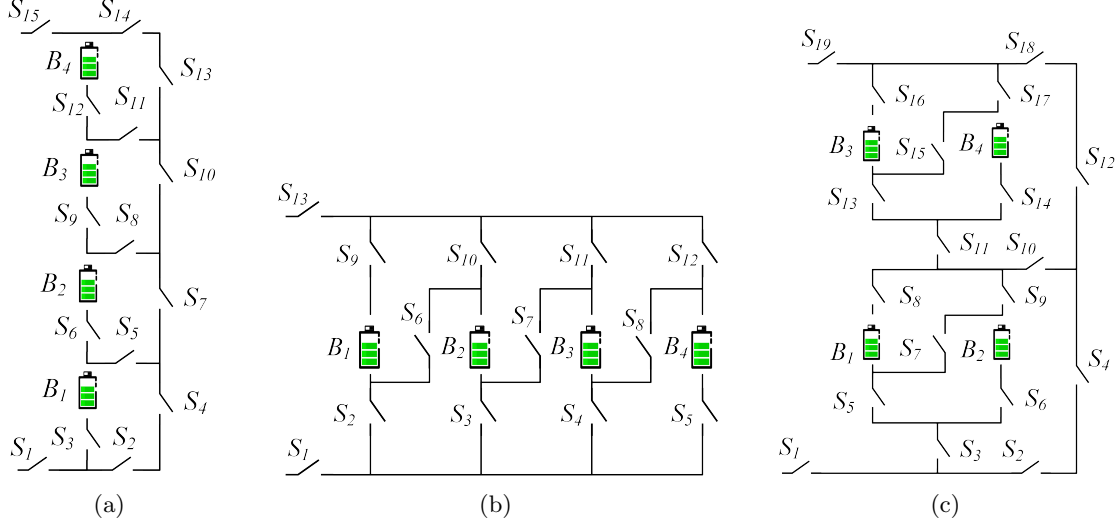


Figure 5: The ~~4-battery-four-battery~~ RBS structures proposed by (a) Lawson [15], (b) Visairo [11], and (c) this paper.

health when the RBS output reaches the MAC. ~~Figure Fig.~~ 6f presents the corresponding circuit, with the red highlight indicating that ~~the~~ current is flowing through the respective branches.

Table 1: ~~Calculated MAC~~ ~~Calculating result of the 4-battery-for four-battery~~ RBS structure in ~~Figure Fig.~~ 5c.

Structure	Figure 5c with 4-four batteries and 19 switches
Switch ON-on	$S_1, S_3, S_5, S_6, S_8, S_9, S_{10}, S_{12}, S_{18}, S_{19}$
I_o	$2u_b/(2R_o + r_b)$
I_b	$[u_b/(2R_o + r_b), u_b/(2R_o + r_b), 0, 0]$
η_{\max} η	2

Similarly, the ~~MAC-calculation~~ results of the ~~structures in Figures~~ ~~MAC calculation for the~~ structures in Figs. 5a and 5b are ~~shown as Table 2 and Table~~ listed in Tabs. 2 and 3, respectively.

To verify and compare the results from the greedy algorithm, we also used a brute-force algorithm that iterates through all possible switch states to calculate the MAC of the same three RBSs. The final results are the same as the results shown in Tabs. 1–3. The method uses the greedy algorithm to calculate 11, 11, and 1 reconfigured structures for the RBS structure in Figs. 5c, 5a, and 5b, respectively. For the same RBS, the method counts all possible switch states, which equates to 2^{19} , 2^{15} , and 2^{13} structures, respectively.

Furthermore, the RBS ~~under the scenario of~~ ~~with~~ isolated batteries is taken into consideration and calculated. The MAC calculation results for the three structures under study, with varying numbers of isolated batteries, are presented in ~~Table 4. Figures 7a-Tab. 4. Figs. 7a-7d~~ illustrate the corresponding ~~switch-control~~ ~~switch-control~~ schemes for the new structure proposed in this paper under different ~~isolated battery conditions~~. The characteristics of these three structures in the

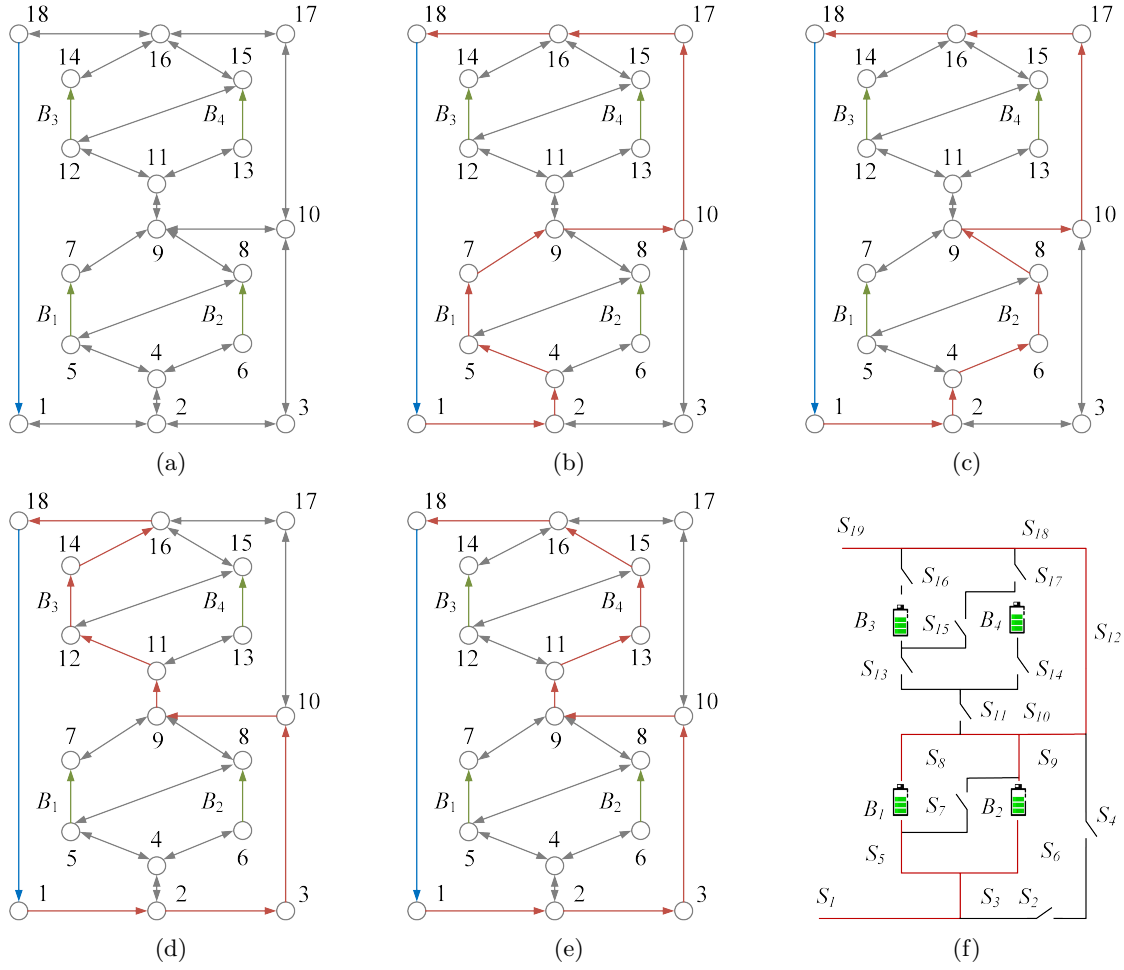


Figure 6: For the RBS structure in Figure 5c, (a) its directed graph and the SPs SPs (high-lighted in red) of battery (b) B_1 , (c) B_2 , (d) B_3 , and (e) B_4 . (f) The circuit of the RBS with its output reaching the MAC.

Table 2: MAC Calculating result of the 4-battery-four-battery RBS structure in Figure 5a.

Structure	Figure 5a with 4 batteries and 15 switches
Switch ON	$S_1, S_3, S_5, S_7, S_{10}, S_{13}, S_{14}, S_{15}$
I_o	$u_b / (R_o + r_b)$
I_b	$[u_b / (R_o + r_b), 0, 0, 0]$
η_{\max}	1

Table 3: MAC Calculating result of the 4-battery-four-battery RBS structure in Figure 5b.

Structure	Figure 5b with 4 batteries and 13 switches
Switch ON	$S_1, S_2, S_3, S_4, S_5, S_9, S_{10}, S_{11}, S_{12}, S_{13}$
I_o	$4u_b / (4R_o + r_b)$
I_b	$[u_b / (4R_o + r_b), u_b / (4R_o + r_b), u_b / (4R_o + r_b), u_b / (4R_o + r_b)]$
η_{\max}	4

context of battery isolation will be discussed in the next subsection conditions of isolated batteries.

Table 4: ~~The variation~~ Variation of MAC with the number of isolated batteries for different RBS structures, including the structure proposed by Lawson et al., Visairo et al., and the structure proposed in this paper.

Number of isolated batteries	η of RBS structure		
	our This paper	Visairo 's	Lawson 's
0	2	4	1
1	2	3	1
2	2 ^a or 1 ^b	2	1
3	1	1	1

^a Isolate two batteries within the same substructure, as shown in Fig. 7b.

^b Isolate one battery in each of the two substructures, as shown in Fig. 7c.

3.3 Discussion

In this subsection, we firstly discuss the correctness of the results presented in Figure 6 and Table 1. Consider first the results shown in Fig. 6f and listed in Tab. 1. When B_1 and B_2 or B_3 and B_4 are connected in parallel, the RBS can output the maximum current, which is $\eta = 2$ (i.e., twice the current output of a single battery in RBS). Adding more batteries to the main circuit can only form a series structure and will not improve the MAC. Therefore, the switches state given in Table 1 can make state of the switches given in Tab. 1 maximizes the RBS output current reach the maximum. The brute-force method, which go through all possible switch states, also gives the same result.

It is important to note that when solving for MAC The literature contains no report on an algorithm for calculating the MAC of an RBS. The brute-force algorithm, which goes through all possible switch states, is the most straightforward way to determine the MAC and is used as a benchmark for the proposed greedy algorithm. If an RBS has N_b batteries and N_s switches and the corresponding directed graph has N nodes, 2^{N_s} iterations are required to traverse all reconfigured structures. Calculating each reconfigured structure using Eqs. (7)–(10) requires matrix inversion and matrix multiplication, which has a time complexity of $O(N^3 + 2N^2N_b + N^2N_s + NN_b^2)$. Therefore, the time complexity of the brute-force algorithm is $O((N^3 + 2N^2N_b + N^2N_s + NN_b^2)2^{N_s})$. The greedy algorithm proposed in this paper requires that SP be found for each battery, which requires N_b iterations. Each SP can be obtained by several applications of Dijkstra's algorithms. Therefore, the total time complexity for calculating all SPs is $O(N_b(N_b + 2N_s) \log_{10} N)$. According to Appendix 1, the RBS can reconfigure $C_{N_b}^{N_{set}}$ structures by selecting N_{set} batteries from N_b batteries, which gives $\sum_{N_{set}=1}^{N_b} C_{N_b}^{N_{set}} / N_b \approx 2^{N_b} N_b^{-1}$ on average. Thus, with the bisection method, the time complexity of the greedy algorithm is $O((N^3 + 2N^2N_b + N^2N_s + NN_b^2)2^{N_b} N_b^{-1} \log_{10} N_b + N_b(N_b + 2N_s) \log_{10} N)$. Based on currently proposed RBS structures [23, 24, 25, 26, 27, 28], the number N_b of batteries, N_s of switches, and N of nodes are quantitatively related as follows: $N_s \approx (3-5)N_b$, $N \approx N_s$. After simplifying, the time complexity of the method with greedy algorithm is $O(2^{N_b} N_s^2 \log_{10} N_b)$, while it is $O(2^{N_s} N_s^3)$ for the method with brute force algorithm. Therefore, as the RBS grows, especially

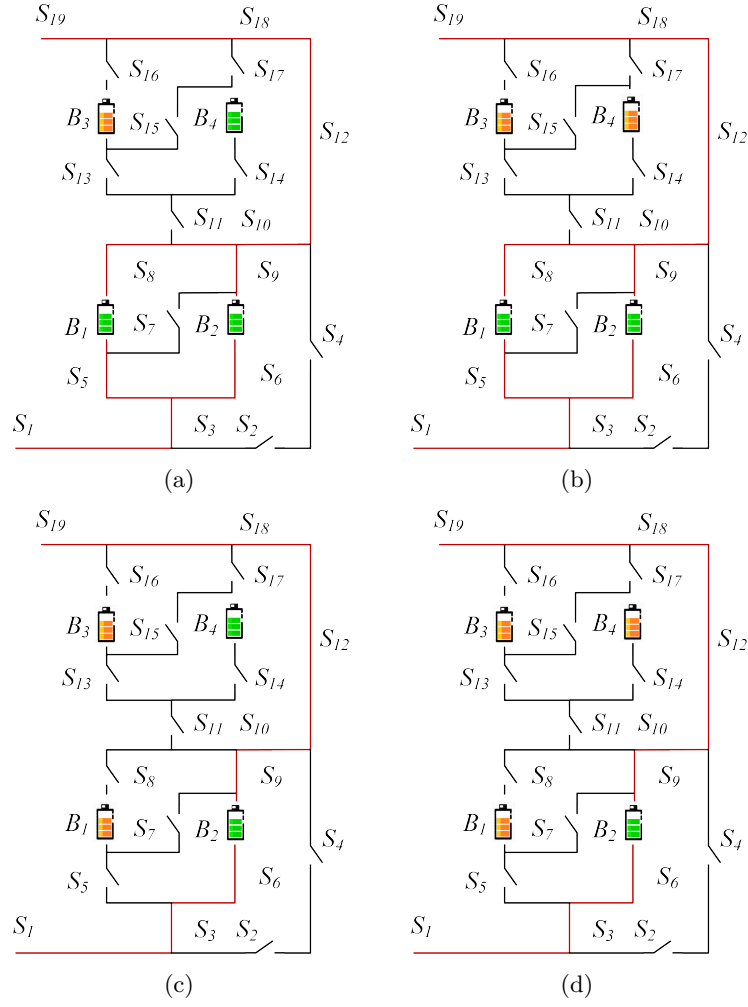


Figure 7: ~~The circuit~~ Circuit states of MACs when isolating (a) one, (b) two (best case), (c) two (worst case), and (d) three batteries for the structure in ~~Figure Fig.~~ Fig. 5c.

in the number of switches, the greedy algorithm gains an advantage over the brute-force algorithm. This is confirmed by the number of structures required to determine the MAC in the previous section. Compared with the brute-force algorithm, the method based on the greedy algorithm is 3 000 to 48 000 times more efficient, which is theoretically $N_s 2^{N_s - N_b} \log_{10} N_b$ times according to the above time-complexity analysis. This benefits from two key points:

- (1) The SPs guide the RBS to reconfigure reasonable structures rather than blindly going through all possible structures. This reduces the complexity from 2^{N_s} to 2^{N_b} , which is the main reason for the improvement in efficiency.
- (2) The bisection method further accelerates this process, reducing the complexity from 2^{N_b} to $2^{N_b} N_B^{-1} \log_{10} N_b$.

However, the greedy algorithm proposed in this paper still contains exponential terms in the time complexity, which means it may not be able to handle extremely large RBS structures having large N_b .

Note that η is used as the objective function instead of I_o in solving for the MAC. This choice makes the ~~result of resulting~~ MAC more reasonable. As shown in ~~Table Tab.~~ 1, I_o and I_b are functions of R_o , u_b , and r_b . ~~If However, when I_o were is~~ used as the objective function, even for the same RBS structure, the MAC ~~result and corresponding switches state solution and corresponding switch states~~ could change due to different external electrical appliances. ~~It This~~ would increase the difficulty and uncertainty ~~in RBS structuredesign. In contrast, by using η as the objective function, which is defined as the ratio of I_o and $\max I_b$, the influence of these factors on the results can be eliminated. η solely reflects of designing the RBS structure. To eliminate this problem, the maximum output current capability of the RBS structure ratio $\eta = I_o / \max I_b$ is adopted as the objective function in our research. Recall that η reflects only the structure's ability to output current, rather than the actual current outputing by the battery system. Assuming that the maximum allowed current MAC of batteries in the RBS is I_m , the maximum output current of the RBS structure can be calculated as ηI_m by determining the η of the structure. Therefore, compared to I_o , value of η is more suitable for structure design for the structure.~~

The method proposed in this paper ~~is significant for facilitates~~ the design of ~~next-generation~~ RBSs in the following ~~aspects. Most of the ways:~~ Most currently proposed RBS structures [23, 24, 25, 26, 27, 28] ~~exhibit have~~ simple topological characteristics, ~~and the calculation of so calculating the~~ MACs is relatively straightforward, even intuitive. However, these simple structures do not always fully satisfy the requirements of complex applications, such as dynamically adapting the circuit to variable and random operating conditions ~~, and or~~ actively equalizing differences ~~among the between~~ batteries in the RBS. Moreover, isolating the batteries disrupts the original regularity and symmetry of the topology, which complicates the otherwise simple structure, and the maximum output current of the system becomes more challenging to obtain. ~~Owing to the advantages of pervasiveness and automation In contrast,~~ the proposed method ~~can be employed to calculate calculates~~ the MAC of arbitrary RBS structures, ~~which helps to address the aforementioned issues and paves the way for more notably the~~ complex and flexible RBS ~~structure design structures~~.

To illustrate this point, the MACs of ~~the three RBS structures mentioned above~~ are calculated after ~~the batteries are isolated~~ isolating one or more of the batteries, as shown in ~~Table Tab.~~ 4. Specifically, for the structure presented in ~~Figure Fig.~~ 5c, the corresponding circuit states ~~of for the~~ MACs when isolating ~~different numbers of one to three~~ batteries are depicted in ~~Figures 7a-Figs.~~ 7a-7d. This structure has two cases ~~of isolating two batteries in which two batteries are isolated:~~ one is to isolate two batteries within the same substructure (~~Figure Fig.~~ 7b), in which case $\eta = 2$; the other is to isolate one battery in each of the two substructures (~~Figure Fig.~~ 7c), in which case $\eta = 1$. ~~From the results, it can be observed. The results in Figs. 7a-7d show that the proposed method provides reasonable outcomes for isolating batteries with any number and position.~~ any number of batteries in any position. Furthermore, the ~~performance of~~ output current for the three ~~RBS when isolating RBSs with isolated~~ batteries is also shown in ~~Table Tab.~~ 4. For the structure proposed by Lawson et al., the MAC ~~remains the same as that without isolated battery cells, i.e., $\eta = 1$, when the is independent of the~~ number of isolated ~~battery cells increases, until all the cells in the RBS are isolated. For batteries.~~ However, for Visairo's structure, the MAC decreases ~~as upon increasing the number of isolated battery cells increases, until $\eta = 0$. In contrast batteries.~~ Nevertheless, the MAC of the structure proposed in this work ~~is positioned between the falls between the MACs of these~~ two structures. This ~~result~~ indicates that the structure proposed in this paper ~~, compared to Lawson's structure, has a larger MAC under than Lawson's for the same number of batteries, which means a wider output current regulation range. On the other hand, by simply changing the states of S_2, S_4, S_{11} , and S_{12} in the conversion structure, this structure can address the majority of battery isolation scenarios, whereas Visairo's structure requires specific battery targeting and switch control. In summary, the structure proposed in this paper has the advantages of both Lawson's and Visairo's structures and has a wider range of regulation of the output current.~~

4 Conclusion

This paper proposes a pervasive and ~~automatic method for computing automated method to~~ efficiently compute the MAC of ~~the given an~~ RBS. The method is implemented by a greedy algorithm combined with ~~a an improved~~ directed graph model, ~~whose effectiveness is tested on a novel and complex RBS structure. The method remains effective for the application scenario of RBS battery isolation and demonstrates that the novel structure has the advantage on flexible output current and convenient battery isolation. Future research could focus on developing new indicators to evaluate the performance.~~ Not only does the method provides the same global MAC calculation results as the brute force method, but it also improves the calculation efficiency by 3 000 to 48 000 times for three RBS structures in the case study. Theoretically, for an RBS with N_s switches and N_b batteries, the efficiency of the proposed method is $N_s 2^{N_s - N_b} \log_{10} N_b$ times that of the brute-force method, which is mainly because of using the batteries' SPs to guide the RBS to reconfigure reasonable structures rather than blindly going through all possible structures. The main advantage of this method is its ability to calculate the MAC of RBSs with arbitrary structures. Even in scenarios with random isolated batteries, the proposed method remains effective. This method helps to fully tap the current output potential of the RBS ~~with the currents and voltages obtained by the method,~~

as well as modifying the equivalent model of the battery to allow for more accurate simulations of the RBS, including transient analysis, guide the RBS structure design and optimization in the design stage, and assist in evaluating the current-overload risk of the system in practical applications.

5 Appendix

Algorithm 1: Get the max available currents of a certain RBS

Data: Directed graph model $G(V, E)$ of the RBS
Result: $\max \eta$

```

1 for  $i \in E_b$  do
2    $P_i \leftarrow \{path | \text{starts at } v_1 \text{ and ends at } v_n\}$ ;
3    $SP_i \leftarrow p_i$  which has the minimum  $\omega(p_i)$  among all  $p_i \in P_i$ .
4 end
5 get  $A$  by Equation Eq. 1;
6 while not yet determine  $\max \eta$  do
7    $N_{set} \leftarrow$  number of selected SPs calculated by dichotomy;  $N_{set} \leftarrow$  number of selected SPs
   calculated by dichotomy;
8    $C_b \leftarrow$  set of all combinations of  $N_{set}$  batteries from  $N_b$ ;  $C_b \leftarrow$  set of all combinations of
    $N_{set}$  batteries from  $N_b$ ;
9   for  $c_b \in C_b$  do
10     $x_s \leftarrow$  list of all switches' state:  $x_s[j] = 1$  if  $j \in \bigcup_{i \in c_b} SP_i$  else 0;
11     $X \leftarrow diag[1, 1, \dots, 1, x_s]$ ;
12    get  $Y_n$  by Eq. 9;
13    if  $Y_n$  is invertible then
14      pass
15    else
16      construct an effective solution
17    end
18    get  $I_o$  by Eq. 7;
19    get  $I_b$  by Eq. 8;
20    if  $\max(I_b) \leq I_m$  then
21       $\eta \leftarrow I_o / \max(I_b)$ ;
22    else
23      break
24    end
25  end
26 end

```

Acknowledgments

Author Contributions

B. Xu conceived the main idea, formulated the overarching research goals and aims, designed the algorithm, and reviewed and revised the manuscript. G. Hua developed and analyzed the model, implemented the code and supporting algorithms, and wrote the initial draft. C. Qian provided

critical review, commentary, and revisions. Q. Xia contributed to shaping the research, analysis, and manuscript. B. Sun conducted the research and investigation process. Y. Ren secured the funding and supervised the project. Z. Wang verified the results and provided necessary resources.

Funding

This work was supported by the National Natural Science Foundation of China (NSFC, No.52075028).

Conflicts of Interest

The authors declare that there is no conflict of interest regarding the publication of this article.

Data Availability

This work does not require any data to be declared or publicly disclosed.

References

- [1] Yuqing Yang, Stephen Bremner, Chris Menictas, and Merlinde Kay. Battery energy storage system size determination in renewable energy systems: A review. *Renewable and Sustainable Energy Reviews*, 91:109–125, August 2018.
- [2] Luanna Maria Silva de Siqueira and Wei Peng. Control strategy to smooth wind power output using battery energy storage system: A review. *Journal of Energy Storage*, 35:102252, March 2021.
- [3] Eugene Schwanbeck and Penni Dalton. International Space Station Lithium-ion Batteries for Primary Electric Power System. In *2019 European Space Power Conference (ESPC)*, pages 1–1. IEEE, September 2019.
- [4] Lihua Zhang. Development and Prospect of Chinese Lunar Relay Communication Satellite. *Space: Science & Technology*, 2021, January 2021.
- [5] Jaephil Cho, Sookyung Jeong, and Youngsik Kim. Commercial and research battery technologies for electrical energy storage applications. *Progress in Energy and Combustion Science*, 48:84–101, June 2015.
- [6] Naixing Yang, Xiongwen Zhang, BinBin Shang, and Guojun Li. Unbalanced discharging and aging due to temperature differences among the cells in a lithium-ion battery pack with parallel combination. *Journal of Power Sources*, 306:733–741, February 2016.
- [7] Fei Feng, Xiaosong Hu, Lin Hu, Fengling Hu, Yang Li, and Lei Zhang. Propagation mechanisms and diagnosis of parameter inconsistency within Li-Ion battery packs. *Renewable and Sustainable Energy Reviews*, 112:102–113, September 2019.

- [8] J. A. Jeevarajan and C. Winchester. Battery Safety Qualifications for Human Ratings. *Interface magazine*, 21(2):51–55, January 2012.
- [9] Daniel Vázquez Pombo. A Hybrid Power System for a Permanent Colony on Mars. *Space: Science & Technology*, 2021, January 2021.
- [10] Weiji Han, Torsten Wik, Anton Kersten, Guangzhong Dong, and Changfu Zou. Next-Generation Battery Management Systems: Dynamic Reconfiguration. *IEEE Industrial Electronics Magazine*, 14(4):20–31, December 2020.
- [11] H. Visairo and P. Kumar. A reconfigurable battery pack for improving power conversion efficiency in portable devices. In *2008 7th International Caribbean Conference on Devices, Circuits and Systems*, pages 1–6. IEEE, April 2008.
- [12] Song Ci, Jiucui Zhang, Hamid Sharif, and Mahmoud Alahmad. A novel design of adaptive reconfigurable multicell battery for power-aware embedded networked sensing systems. In *IEEE GLOBECOM 2007-IEEE Global Telecommunications Conference*, pages 1043–1047. IEEE, 2007.
- [13] Jan Engelhardt, Tatiana Gabderakhmanova, Gunnar Rohde, and Mattia Marinelli. Reconfigurable stationary battery with adaptive cell switching for electric vehicle fast-charging. In *2020 55th International Universities Power Engineering Conference (UPEC)*, pages 1–6, 2020.
- [14] Jan Engelhardt, Jan Martin Zepter, Tatiana Gabderakhmanova, Gunnar Rohde, and Mattia Marinelli. Double-string battery system with reconfigurable cell topology operated as a fast charging station for electric vehicles. *Energies*, 14(9):2414, 2021.
- [15] Barrie Lawson. A Software Configurable Battery. *EVS26 International Battery, Hybrid and Fuel Cell Electric Vehicle Symposium*, 2012.
- [16] Liang He, Linghe Kong, Siyu Lin, Shaodong Ying, Yu Gu, Tian He, and Cong Liu. Reconfiguration-assisted charging in large-scale lithium-ion battery systems. In *2014 ACM/IEEE International Conference on Cyber-Physical Systems (ICCPS)*, pages 60–71. IEEE, 2014.
- [17] Hahnsang Kim and Kang G Shin. On dynamic reconfiguration of a large-scale battery system. In *2009 15th IEEE Real-Time and Embedded Technology and Applications Symposium*, pages 87–96. IEEE, 2009.
- [18] Weiji Han, Anton Kersten, Changfu Zou, Torsten Wik, Xiaoliang Huang, and Guangzhong Dong. Analysis and estimation of the maximum switch current during battery system reconfiguration. *IEEE Transactions on Industrial Electronics*, 69(6):5931–5941, 2021.
- [19] Si-Zhe Chen, Yule Wang, Guidong Zhang, Le Chang, and Yun Zhang. Sneak Circuit Theory Based Approach to Avoiding Short-Circuit Paths in Reconfigurable Battery Systems. *IEEE Transactions on Industrial Electronics*, 68(12):12353–12363, 2021.

- [20] Liang He, Lipeng Gu, Linghe Kong, Yu Gu, Cong Liu, and Tian He. Exploring Adaptive Reconfiguration to Optimize Energy Efficiency in Large-Scale Battery Systems. In *2013 IEEE 34th Real-Time Systems Symposium*, pages 118–127, December 2013.
- [21] Hongwen He, Rui Xiong, Xiaowei Zhang, Fengchun Sun, and JinXin Fan. State-of-Charge Estimation of the Lithium-Ion Battery Using an Adaptive Extended Kalman Filter Based on an Improved Thevenin Model. *IEEE Transactions on Vehicular Technology*, 60(4):1461–1469, May 2011.
- [22] S.M. Mousavi G. and M. Nikdel. Various battery models for various simulation studies and applications. *Renewable and Sustainable Energy Reviews*, 32:477–485, April 2014.
- [23] Song Ci, Jiucui Zhang, Hamid Sharif, and Mahmoud Alahmad. A Novel Design of Adaptive Reconfigurable Multicell Battery for Power-Aware Embedded Networked Sensing Systems. In *IEEE GLOBECOM 2007-2007 IEEE Global Telecommunications Conference*, pages 1043–1047, November 2007.
- [24] Mahmoud Alahmad, Herb Hess, Mohammad Mojarradi, William West, and Jay Whitacre. Battery switch array system with application for JPL’s rechargeable micro-scale batteries. *Journal of Power Sources*, 177(2):566–578, March 2008.
- [25] Hahnsang Kim and Kang G. Shin. Dependable, efficient, scalable architecture for management of large-scale batteries. In *Proceedings of the 1st ACM/IEEE International Conference on Cyber-Physical Systems, ICCPS ’10*, pages 178–187, New York, NY, USA, April 2010. Association for Computing Machinery.
- [26] Younghyun Kim, Sangyoung Park, Yanzhi Wang, Qing Xie, Naehyuck Chang, Massimo Poncino, and Massoud Pedram. Balanced reconfiguration of storage banks in a hybrid electrical energy storage system. In *2011 IEEE/ACM International Conference on Computer-Aided Design (ICCAD)*, pages 624–631, November 2011.
- [27] Taesic Kim, Wei Qiao, and Liyan Qu. A series-connected self-reconfigurable multicell battery capable of safe and effective charging/discharging and balancing operations. In *2012 Twenty-Seventh Annual IEEE Applied Power Electronics Conference and Exposition (APEC)*, pages 2259–2264, February 2012.
- [28] Liang He, Linghe Kong, Siyu Lin, Shaodong Ying, Yu Gu, Tian He, and Cong Liu. Reconfiguration-assisted charging in large-scale Lithium-ion battery systems. In *2014 ACM/IEEE International Conference on Cyber-Physical Systems (ICCPS)*, pages 60–71, April 2014.